Journal of the Korean Society of Surveying, Geodesy, Photogrammetry and Cartography
Vol. 38, No. 2, 123-130, 2020
https://doi.org/10.7848/ksgpc.2020.38.2.123

ISSN 1598-4850(Print)
ISSN 2288-260X(Online)
Original article

Evaluating Tropical Night by Comparing Trends of Land cover and Land Surface Temperature in Seoul, Korea

Sarker, Tanni[1] · Huh, Jung Rim[2] · Bhang, Kon Joon[3]

Abstract

The impact of urbanization on LST (Land Surface Temperature) and TN (Tropical Night) was observed with the analyses of land cover change and LST by associating with the frequency of TN during the period of 1996 to 2016. The analyses of land cover and LST was based on the images of Landast 5 and 8 for September in 1996, 2006, and 2016 at a 10 year interval. The hourly-collected atmospheric temperatures for the months of July and August during the period were collected from AWSs (Automatic Weather Stations) in Seoul for the frequency analysis of TN. The study area was categorized into five land cover classes: urban or built-up area, forest, mixed vegetation, bare soil and water. It was found that vegetation (-7.71%) and bare soil (-9.04%) decreased during the period while built-up (17.29%) area was expanded throughout the whole period (1996-2016), indicating gradual urbanization. The changes came along with the LST rise in the urban area of built-up and bare soil in Seoul. In addition, the frequency of TN has increased in 4.108% and 7.03% for July and August respectively between the two periods of the 10 year interval, 1996-2006 and 2006-2016. By comparing the increasing trends of land cover, LST, and TN, we found a high probability that the frequency of TN had a relationship with land cover changes by the urbanization process in the study area.

Keywords : Tropical Night, Surface Temperature, Land Cover, Remote Sensing, Surface Change

1. Introduction

As population increases and city develops, transforming the nature into a human-friendly environment is indispensible. For a long time, various efforts have been made to create an ideal city optimized for humans. In the modern era, human beings started to build large-scale buildings for residence and made many modifications for efficient transportation and buildings optimized for human life. In response to these urban changes, analyses of urban changes have been conducted, and accurate and timely change detection has become very important for a well-planned and sustainable urban development (Lu *et al*., 2004). These human activities changed the urban thermal environment and caused several critical issues (Ye *et al*., 2010; Li *et al*., 2010) such as UHI (Urban Heat Island). UHI refers to the phenomenon that the atmospheric temperature in urban areas is higher than that of the rural (Howard, 1883; Oke, 1982; Taha, 1997; Tran *et al*., 2017).

UHIs not only affect biodiversity by reducing primary production in the ecosystem due to changes in land cover, but also deteriorate air quality (Ronsenfeld *et al*., 1995) by increasing the concentration of ozone and fine dust in the atmosphere caused hazardous environment for the public (Changnon *et al*., 1996) and inducing more energy consumption for cooling which consequently increases the green house gases released to the atmosphere. These work as a chain producing a negative effect to all living organisms so

Received 2020. 03. 19, Revised 2020. 04. 06, Accepted 2020. 04. 29
1) Dept. of Geography, M.S. student, George Washington University (E-mail: tanni.aust@gmail.com)
2) Senior scientist, Social Eco Tech Institute, Konkook University (E-mail: jr529@naver.com)
3) Corresponding Author, Member, Professor, Dept. of Civil Engineering, Kumoh National Institute of Technology (E-mail: bhang.1@kumoh.ac.kr)

that UHI increases the incidence of heat-related diseases and violence by humans due to heat stress (Santamouris *et al*., 2001; O'Loughlin *et al*., 2012).

Unfortunately, there is no practical way to accurately and quantitatively measure the heat balance of the entire urban area for UHI. For example, heights of AWSs (Automatic Weather Stations) in a city should be located at the same level from the ground but they have various heights and usually distributed unevenly and sparsely so that the datasets include inherent bias or discrepancy from the actual measurement values to be expected at the same level (Fujibe, 2009; Wang *et al*., 2015). Researchers, therefore, attempted to understand possible causing factors of UHI by comparing various datasets collected from different sensors. As an alternative, urban heat island intensity has been often used as to meausre the temperature difference between the urban and rural areas (Kim and Baik, 2004). Although the causes of UHI are often described by land cover changes such as vegetation loss and man-made structures in urban areas, studies are still underway to solidify the basis of direct causes and effects on UHI.

Despite the limitations, researchers accepted that surface temperature is correlated with the properties of land covers (Quattrochi and Luvall, 1999) and that urbanization is one of the driving forces contributing to UHI (Kalnay and Ming, 2003).

Interestingly, UHI often accompany with the temperature rise typically at nighttime, termed by TN. TN is the phenomenon in which daytime heat absorbed into the ground is released and trapped by atmospheric water vapor during nighttime in the atmosphere so that the average minimum temperature at nighttime exceeds a specific value of temperature (Alexander *et al*., 2006) which is 25°C in Korea (Choi and Kwon, 2005; Ha and Yun, 2011). Interestingly, TN was attributed as an increasing trend of the atmopsheric temperature during nighttime typically in large cities over past 40 years from 1951 (Karl *et al*., 1991; Choi, 2004). The increase trend is particularly true in July and August in cities of Korea and includes the possibility of rapid cover change in Daegu and Busan during the last 50 years (Suh and Kim, 2015). Choi and Kwon (2005) showed that the evening TN generally occurs in cities at low latitude inland areas due to UHI and late and early morning TN are affected by the thermal inertia of the warm ocean. This fact widely opened the possibility of the impact of urbanization in large cities in terms of environmental influences by land cover changes.

The rapid increase in TNs in large cities such as Seoul has emerged as an important environmental issue along with global warming. In particular, it is believed that the phenomenon of TN at night is believed to have a strong relationship with the spatial distribution of urban land cover as a part of urban heat islands, but studies of direct comparison of TN and land cover change are rarely conducted typically with the remote sensing approach. Therefore, we compared the relationship between urban heat distribution on the ground surface according to the change of land covers in Seoul and atmospheric temperature datasets. This study includes comprehensive analysis on land cover changes on Septembers in 1996, 2006 and 2016 to identify the urbanization process in Seoul and the relationship between the two factors of the urbanization of Seoul and the frequency of TN was compared to evaluate whether the urbanization trend has the same trend as the frequency of TNs during this period.

2. Methodology

2.1 Study area

The study area covers Seoul and its surrounding areas as shown in Fig. 1. Seoul is one of the largest cities in the world with packed high-rise buildings and large population and distinguished by cold and dry winter and hot humid summer with the annual average temperature of 12.2°C. August is considered as the hottest month and the average temperature of the month is around 30°C in summer so UHI is distinct and causes environmental issues such as fine dust and TN. Seoul has experienced urbanization typically from 1960 to 1990 and is still expanding to its neighboring areas so the green area including parks occupies around 30% out of the total area of Seoul. We included the surrounding area of Seoul because Seoul itself does not include a small portion of vegetation covers so that land cover transform might not distinguishable.

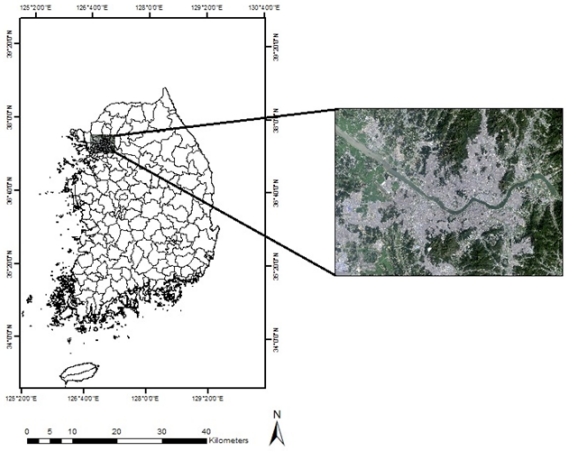

Fig. 1. Study area

2.2 Data acquisition

For spatial analyses on land cover and LST, we obtained Landsat images in the L1T (Level 1 Terrain corrected) format from EartheExplorer (https://earthexplorer.usgs.gov/) by USGS (U.S. Geological Survey). All images are georeferenced to the UTM (Universal Transverse Mercator) coordinate system with the WGS84 datum. Seoul and its vicinity is commonly located on the path 116 and row 34 of Landsat 5 and 8.

Three Landsat satellite images (Table 1) of Septembers in 1996, 2006, and 2016 were used for land cover classification and surface temperature extraction. Because Landsat 7 ETM+ (Enhanced Thematic Mapper Plus) had an operational issue of Scan Line Corrector, which generated strips with no data, we used Landsat 5 TM (Thematic Mapper) and Landsat 8 OLI (Operational Land Imager) and TIRS (Thermal Infra-Red Sensor) images. During the summer months from July to September of 1996, 2006, 2016, the image should satisfy the image selection criteria of minimum cloud covers and temporal variations, Thus, available Landsat images of the years were the images of TM on Sep. 1, 1996 and Sep. 13, 2006 and TIRS on Sep. 24, 2016.

To compare land cover change with the frequency of TNs in Seoul, meteorological data were retrieved from 25 Automatic Weather Stations (AWS) by the Korean Meteorological Administration (KMA) from 1996 to 2016.

2.3 Data processing

Fig. 2 shows the scheme of the data processing for land cover classification and land surface temperature.

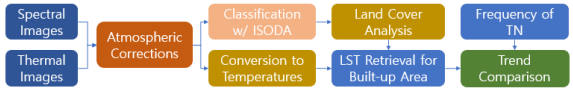

Fig. 2. Scheme of data processing

As a first step, the Landsat images are corrected using the FLAASH module in the ENVI software package. It is incorporated with the MODTRAN (MODerate resolution atmospheric TRANsmission) radiation transfer code and automatically derives the reflectance values from pixel digital numbers of the spectral images. ACPC (Atmospheric Correction Parameter Calculator) from NASA was also employed to extract atmospheric parameters such as transmission, up- and down-welling radiances for thermal images of TM. Note that ACPC is a web-based parameter calculator for the atmospheric correction of thermal bands of Landsat 5, 7, and 8 by NASA (https://atmcorr.gsfc.nasa.gov). Then, the representative emissivity values of 0.98 was inserted for the land surface temperature calculation since the pixel emissivity over urban areas typically ranges from 0.96 to 0.98. Band 11 of TIRS was not used because the error of band 10 of TIRS is a half of that of band 11 by SLA (Stray Light Anomaly) that is termed as the affection by thermal energy outside the field of view. Detailed information about

Table 1. Information of Landsat images

Sensor	Spatial Resolution	Acquisition (yyyy/mm/dd)	Path/Row	Cloud (%)
TM	30m	1996/09/01	116/034	0
TM	30m	2006/09/13	116/034	0
OLI (TIRS)	30m (100m)	2016/09/24	116/034	0

SLA is beyond of the scope of this study but can be found at https://usgs.gov/land-resources/nli/landsat/landsat-8-oli-and-tirs-calibration-notices.

Types of land covers were categorized into five classes, water bodies, dense vegetation such as forest, mixed vegetation with the ground, built-up area fully covered by man-made structures (i.e., pavements and buildings), and bare soil including rocks. Among several classification schemes, we adopted the ISODATA classification scheme because it is simple and can partially implement a supervised classification procedure that can increase the classification accuracy. The study area was segmented into 100 classes and each class was merged into one of the five classes by identifying actual land cover types with reference maps such as photographs from National Geographic Information Institute. Some classified areas, however, were still unidentifiable and, in this case, they were belonged to a miscellany class which was not included in this study. After classification, the classification accuracy was evaluated with producer's and user's accuracies and kappa coefficients (Campbell and Wynne, 2011) by selecting 300 random pixels and subsequently compared against the reference. To perform the analysis on land cover change, LCM (Land Change Modeler) was integrated with the IDRISI software (Eastman, 2006), an advanced analytical tool of land mapping and analysis allowing faster, automated, and comprehensive analysis of land cover change.

3. Results and Analysis

3.1 Classification accuracy

An error matrix was created in a standard tabular form to present classification errors (Table 2). The overall accuracies of classified images (1996, 2006, 2016) were 90.8%, 91.6% and 94.0 with kappa coefficients of 0.88, 0.89, and 0.92, respectively. The accuracies were better than the USGS accuracy level of 85% for land use/cover classification with Landsat (Anderson *et al*., 1976).

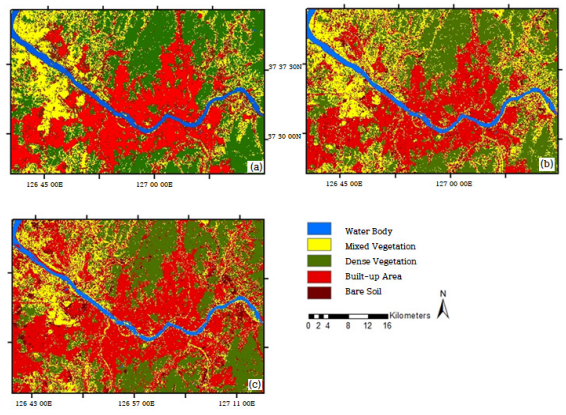

Fig. 3. Classification results of (a) 1996, (b) 2006, and (c) 2016

3.2 Land cover change

The land covers of the study area were analyzed to quantify changes of the study area from 1996 to 2016 in two different ways, overall coverages and gain and loss for each land cover. Fig. 3 shows the basic classification results that the area had undergone. There are noticeable changes in three land covers of mixed vegetation, dense vegetation and built-up area and the built-up area typically increased with the ratios from 24.5% in 1996 to 41.8% in 2016. On the other hand, water body, dense vegetation, bare soil all decreased for the period. The overall trend can be described as the built-up area was expanding during the period from 1996 to 2016.

Table 2. Accuracies of land covers in the study area

	User's Accuracy (%)					Producer's Accuracy (%)					OA (%)	KC
Year	WB	BA	BS	DV	MV	WB	BA	BS	DV	MV		
1996	86.7	92.1	90.3	93.5	89.7	96.3	83.4	94.2	93.6	86.0	90.8	0.88
2006	86.7	86.8	93.1	95.2	91.7	96.3	86.8	91.8	95.2	88.0	91.6	0.89
2016	96.4	92.5	92.0	96.7	93.6	93.1	92.5	97.2	93.5	89.8	94.0	0.92

※ WB=Water Body, BA=Built-up Area, BS=Bare Soil, DV=Dense Vegetation, MV=Mixed Vegetation, OA=overall accuracy, KC=kappa coefficient

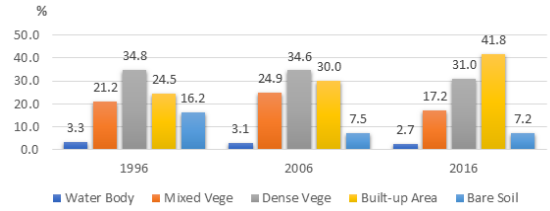

Fig. 4. Ratios of land covers in the study area for 1996, 2006, and 2016

The further analysis showed more details about the gain and loss for each land cover during the study period (Fig. 4). The built-up area gained 250.7 km^2 more than 3 times of the loss (77.1 km^2) from 1996 to 2006. the same gain and loss pattern was found from 2006 to 2016. The mixed vegetation and bare soil from 1996 to 2006 worked in the opposite way so that gain and loss were exceeded to those of the built-up area. This gain and loss pattern was the same as those in the next 10 years from 2006 to 2016 but the net gain was much higher that the previous period. However, the facts does not indicate that the major receptors and donators for the changes.

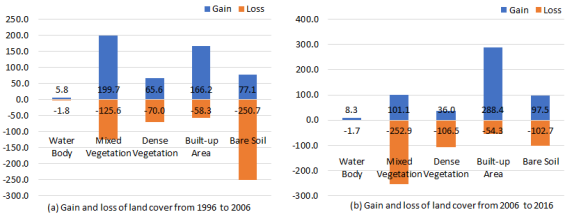

Fig. 5. Gains and losses of land cover during two decades (1996-2016) (Unit: km^2)

A detailed analysis was shown in Fig. 5 to describe how much each land cover was contributed to other land covers for the period of 1996 to 2006. It can be identified that the bare soil lost a large area mostly to the built-up and mixed vegetation areas (90.93 km^2 and 75.47 km^2, respectively). However, the mixed vegetation only received 8.95 km^2 from the built-up area. In other words, the mixed vegetation was the most susceptible land cover type during this time. The interesting facts are the built-up area was the only acceptor even though the bare soil was the only donator to all the other land covers. It is a natural process that bare soil is transformed to mixed vegetation and with human activity, the cover is the most likely area that can be easily developed. These findings were the same to the period from 2006 to 2016, which means urbanization was still be in progress and may keep involving in the same issues at least caused by urbanization in the study area as described in the previous section. In Fig. 5, the water body and dense vegetation did not change much and may hardly influence on the urbanization process.

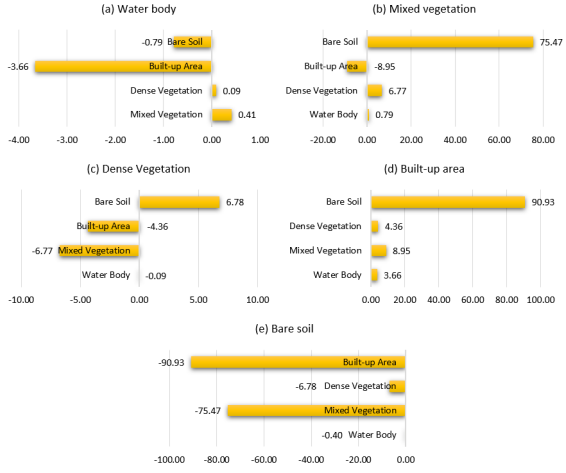

Fig. 6 . Contributions to other land covers from 1996 to 2006 (km^2)

3.3 Comparison of land cover with LST

The LST by land cover types has been compared to understand the characteristics in Seoul. Seoul is noticeably featured by high density of concrete and asphalt materials, the built-up area, so higher temperature in these areas was expected than other land covers. Table 3 shows that the built-up area had the highest average temperature in Seoul, followed by bare soil, mixed vegetation, dense vegetation and water body. The average LST for the built-up area was found 27.0˚C in 1991 and changed to 27.8˚C and 28.5˚C in 2006 and 2016, respectively. There were an upward trend for the built-up area over the twenty years. LST of the bare soil cover faced a rapid increase by 3.0˚C for 20 year because some of the area included rock which is a high capacity holding heat. The mixed vegetation was 23.4˚C in 1996 and kept increasing for the next years of 2006 and 2016. Note that the mixed vegetation was the area with sparse vegetation mixed with the bare soil so that it was relatively lower than the bare soil.

Table 3. Land surface temperature by land cover type

	1996	2006	2016	ΔT (˚C) (2006-1996)	ΔT (˚C) (2016-2006)
Water body	20.5±0.7	20.8±0.9	21.4±0.6	0.3	0.6
Built-up area	27.0±1.4	27.8±1.9	28.5±1.4	0.8	0.7
Dense vegetation	21.8±1.1	22.2±1.7	22.1±1.2	0.4	-0.1
Mixed vegetation	23.4±1.2	25.4±1.9	26.4±1.1	2.0	1.0
Bare soil	25.1±1.6	27.2±2.1	28.4±1.7	2.1	1.2

The LST for dense vegetation increased by 0.3˚C and did not change significantly over the study period. From the analysis, we could expect that Seoul was being exposed to gradual heat emission from the urban surface influencing the atmospheric condition during 1996 to 2016. The influence by the mixed vegetation and bare soil were relatively small to the built-up area because of their sizes smaller that the built-up area. An interesting fact can be inferred from Table 3 that the average temperature of the built-up area was lower than mixed vegetation and bare soil. This is because the regulation by the government defined rooftops of buildings should be painted with the green color, significantly reducing the thermal heat absorption and emission by buildings like dense vegetation.

The influence of land cover changes on land surface temperature can be understood best by exploring the correlation between thermal signatures and land cover categories (Weng, 2001) as land surface temperature pattern and land cover distribution maintains a strong correlation between them (Tran *et al*., 2017). Fig. 7 illustrates that land surface temperatures for all land covers had an increasing trend for the years, which indicates the possibility of the impact by urban expansion to temperature rises on the surface and possibly in the atmosphere as described in Ren, *et al*., 2007.

As a result, non-transpiring and intensely heated surface of concrete, asphalt and steel took place of traditional wooden houses, rice straw roofs (Xiao and Weng, 2007). These surfaces consume excess heat than they reflect it which contributes increment in both surface and ambient temperature (Ahmed *et al*., 2013).

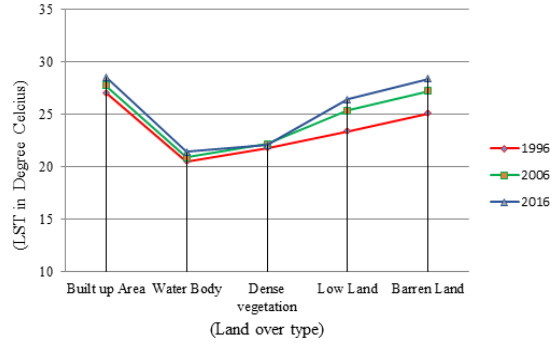

Fig. 7. Variations of average LSTs over different land covers

3.4 Influence of the urban land cover on TN

The frequency of TN was extracted from the daily minimum temperature data from AWSs in Seoul. Fig. 8 and 9 display the frequencies of TN for July and August during two decades, from 1996 to 2006 and from 2006 to 2016, respectively. TN occurred 9.67% and 15.83% out of the total days for July and August from 1996 to 2006, respectively. The ratios were changed to 13.78% and 22.86% for the same months during the next 10 years from 2006 to 2016.

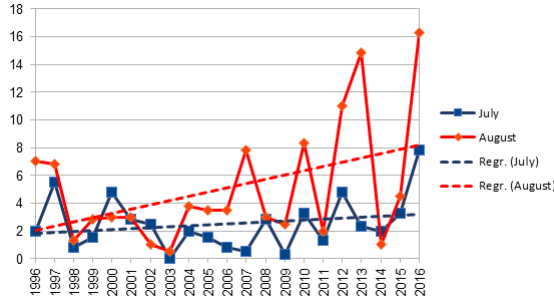

Fig. 8. Trends of the frequency of TN for last 20 years

The upward trend of the frequency from 1996 to 2016 in Fig. 8 is strongly supported by the changes of land cover and surface temperature. In other words, the frequency trend of TN can be described to accompany with the change of land cover, typically the built-up area, in Seoul.

4. Summary and Conclusion

The relationship of the frequency of TN and the changes of land cover and LST in Seoul was investigated over 20 years (1996-2016). During the period, Seoul and its surrounding area experienced on-going urbanization and the thermal environment was suspected to be modified by the urbanization in Seoul and its surrounding area. It suggests that the changes of environmental components are interrelated with the change of land covers. The findings of this study can be summarized like the followings; (1) the study area experienced gradual urbanization from 1996 to 2016 and the built up area was nearly doubled in size between 1996 and 2016 which resulted in significant loss of shallow vegetation and bare soil cover. Bare soil and vegetation covers 190 km^2 were transformed into the built-up area as major contributors to the urbanization in the study area. (2) Land surface temperature increment (0.10°C/10 years) was largely attributed to the rapid growth of the urbanization. The surface temperature was observed comparatively with respect to built-up area and gradual increasing trend was found with the urbanization. (3) The effect of urbanization could be highlighted with the frequency of TN. Since the frequency had a gradually increasing trend for July and August during the period, we concluded that there is a high probability that the frequency of TN had a relationship with land cover changes by the urbanization process in the study area.

Acknowledgment

The study was supported by Research Fund of Kumoh National Institute of Technology

References

Ahmed, B., Kamruzzaman, M., Zhu, X., Rahman, M.S., and Choi, K. (2013), Simulating land cover changes and their impacts on land surface temperature in Dhaka, Bangladesh, *Remote Sensing*, Vol. 5, No. 11, pp. 5969–5998.

Alexander, L.V., Zhang, X., Peterson, T.C., Caesar, J., Gleason, B. Klein Tank, A.M.G., Haylock, M. Collins, D., Trewin, B., Rahimzadeh, F., Tagipour, A., Rupa Kumar, Revadekar, J., Griffiths, G, Vncent, L., Stephenson, D.B., Burn, J., Aguilar, E., Brunet, M., Taylor, M., New, M., Zhai, P., Rusticucci, M., and Vazquez-Aguirre, J.L. (2006), Global observed changes in daily climate extremes of temperature and precipitation, *Journal of Geophysical Research: Atmospheres*, Vol. 111, No. 5, pp. 1–22.

Anderson, J.R., Hardy, E.E., Roach, J.T., Witmer, R.E., and Peck, D.L. (1976), A land use and land cover classification system for use with remote sensor data, *Geological Survey Professional Paper* 964, U.S. Geological Survey, Virginia, USA.

Campbell, J.B. and Wynne, R.H. (2011), *Introduction to Remote Sensing*, The Guilford Press, New York, USA.

Changnon, S.A, Kunkel, K.E., and Reinke, B.C. (1996), Impacts and responses to the 1995 heat wave: A call to action, *Bulletin of the American Meteorological Society*, Vol. 77, No. 7. pp. 1497–1506.

Choi, Y. (2004), Trends on temperature and precipitation extreme events in Korea, *Journal of the Korean Geographical Society*, Vol. 39, No. 5, pp. 711–721.

Choi, G. and Kwon, W.T. (2005), Spatial-temporal patterns and recent changes of tropical night phenomenon in South Korea, *Journal of the Korean Geogrphical Society*, V. 40, No. 6, 730-747. (in Korean with English abstract)

Eastman, J.R. (2006), IDRISI 15.0: *The Andes ed*. Clark University, Worcester, MA, the United States.

Fujibe, F. (2009), Detection of urban warming in recent temperature trends in Japan, *International Journal of Climatology*, Vol. 29, no. 12, pp. 1811-1822.

Ha, K.J. and Yun, K.-S. (2011), Climate change effects on tropical night days in Seoul, Korea, *Theoretical and Applied Climatology*, Vol. 109, pp. 191–203.

Howard, L. (1883), The climate of London: deduced from meteorological observations, made at different places in the neighbourhood of the metropolis, Climate of London, London, pp. 1818-1820.

Kalnay, E. and Ming, C. (2003), Impact of urbanization and land-use change on climate, *Nature*, Vol. 423, pp. 528–531.

Karl, T.R., Kukla, G., Razuvayev, V.N., Changery, M.J. Quayle, R.G., Heim, R.R., Easterling, D.R., and Fu, C.B. (1991), Global warming: evidence for asymmetric diurnal temperature change, *Geophysical Reaserch Letters*, Vol. 18, No. 12, pp. 2253–2256.

Kim, Y.H. and Baik, J.J. (2004), Daily maximum urban heat island intensity in large cities of Korea, *Theoretical and Applied Climatology*, Vol. 79, pp. 151–164.

Li, X., Chen, F Ye, H., Xiong, Y, Shi L., Pan, L., and Wang, K. (2010), Trends of maximum temperature, minimum temperature and diurnal temperature range and their correlations with urbanisation in Xiamen, China, *International Journal of Susteatinable Development and World Ecology*, Vol. 17, No. 4, pp. 299–303.

Lu, D., Mausel, P., Brondizio, E.S., and Moran, E. (2004), Change detection techniques, *International Journal of Remote Sensing*, Vol. 25, No. 12, pp. 2365–2401.

Oke, T.R. (1982), The energetic basis of the urban heat island, *Quarterly Journal of the Royal Meteorological Society*, Vol. 108, No. 455, pp. 1–24.

O'Loughlin, J., Witmer, F.D.W., Linke, A.M., Laing, A., Gettelman, A., and Dudhia, J. (2012), Climate variability and conflict risk in East Africa, 1990-2009, *Proceedings of the National Academy of Sciences*, Vol. 109, no. 45, pp. 18344-18349.

Quattrochi, D.A. and Luvall, J.C. (1999), Thermal infrared remote sensing for analysis of landscape ecological processes: methods and applications, *Landscape Ecology*, Vol. 14, No. 6, pp. 577–598.

Ren, G.Y., Chu, Z.Y., Chen, Z.H., and Ren, Y.Y. (2007), Implications of temporal change in urban heat island intensity observed at Beijing and Wuhan stations, *Geophysical Research Letter*, Vol. 34, No. 5, pp. 1–5.

Rosenfeld, A.H., Akbari, H., Bretsz, S., Fishman, B.L., Kurn, D.M., Sailor, D., and Taha, H. (1995), Mitigation of urban heat islands: materials, utility programs, updates, *Energy and Buildings*, Vol. 22, No. 3, pp. 255–265.

Santamouris, M., Papanikolaou, N., Livada, I., Koronakis, I., Georgakis, C., Argiriou, A., and Assiakopoulos, D.N. (2001), On the impact of urban climate on the energy consumption of buildings, *Solar Energy*, Vol. 70, no. 3, pp. 201-216.

Suh, M.-S. and Kim, C. (2015), Change-point analysis of tropical night occurrences for five major cities in Republic of Korea, *Advances in Meteorology*, Vol. 2015, pp. 1-11, Article ID: 801981.

Taha, H. (1997), Urban climates and heat islands: albedo, evapotranspiration, and anthropogenic heat, *Energy and Buildings*. Vol. 25, No. 2, pp. 99–103.

Tran, D.X., Pla, F, Lattorre-Carmona, P., Myint, S.W., Caetano, M., and Kieu, H.V. (2017), Characterizing the relationship between land use land cover change and land surface temperature, *ISPRS Journal of Photogrammetry and Remote Sensing*, Vol. 124, pp. 119–132.

Wang, J., Huang, B., Fu, D., and Atkinson, P. (2015), Spatiotemporal variation in surface urban heat island intensity and associated determinants across major chinese cities, *Remote Sensing*, Vol. 7, no. 4, pp. 3670-3689.

Weng, Q. (2010), A remote sensing? GIS evaluation of urban expansion and its impact on surface temperature in the Zhujiang Delta, China, *International Journal of Remote Sensing*, Vol. 22, No. 10, pp. 1999–2014.

Xiao, H. and Weng, Q. (2007), The impact of land use and land cover changes on land surface temperature in a karst area of China, *Journal of Environmental Management*, Vol. 85, No. 1, pp. 245–257.

Ye, H., Wang, K., Huang, S., Chen, F., Xiong, Y., and Zhao, X. (2010), Urbanisation effects on summer habitat comfort: a case study of three coastal cities in southeast China, *International Journal of Susteatinable Development and World Ecology*, Vol. 17, No. 4, pp. 317-323.